

## HYDROGENATION OF MgAl FILMS IN PLASMA

L. Pranevičius<sup>a</sup>, D. Milčius<sup>b</sup>, and L.L. Pranevičius<sup>a,b</sup>

<sup>a</sup> Vytautas Magnus University, Vileikos 8, LT-44404 Kaunas, Lithuania  
E-mail: Liudvikas\_Pranevicius@fc.vdu.lt

<sup>b</sup> Lithuanian Energy Institute, Breslaujos 3, LT-44403 Kaunas, Lithuania

Received 26 May 2004

*Dedicated to the 100th anniversary of Professor K. Baršauskas*

Hydriding of MgAl films has been performed in two ways: (i) ion implantation of 100 eV hydrogen ions into the growing film, and (ii) hydrogenation of Mg<sub>17</sub>Al<sub>12</sub> films under high-flux, low-energy hydrogen ion irradiation in H<sub>2</sub>+Ar plasma. The X-ray diffraction studies of phase transitions and structure modifications were carried out. The samples, which were hydrogenated by ion implantation during the deposition of MgAl film, show magnesium alanate, Mg(AlH<sub>4</sub>)<sub>2</sub>, phase. It decomposes at temperatures above 80 °C. The samples hydrogenated in H<sub>2</sub>+Ar plasma show Mg(AlH<sub>4</sub>)<sub>2</sub>, Mg<sub>2</sub>Al<sub>3</sub>, MgH<sub>2</sub>, and Al phases. It is concluded that sputtering induced by Ar ion bombardment during hydrogenation in H<sub>2</sub>+Ar plasma limits the supply rate of hydrogen from the surface into the bulk. Experimentally registered synthesis of new phases and restructuring are explained on the basis of long-range transport of metal species, and the role of grain boundaries is emphasized in the mechanism of hydriding.

**Keywords:** hydrogen storage, hydrides, physical vapour deposition, X-ray diffraction

**PACS:** 68.55.Ln, 68.55.Nq, 34.50.Dy

### 1. Introduction

The use of metallic materials in hydrogen storage and energy conversion technology demands not only a large storage capacity but also large hydrogen bulk diffusivity. A detailed knowledge of the microscopic mechanisms of hydrogen motion is required. The situation becomes even more complex with regard to hydrogen transportation in intermetallic compounds with crystalline grains in the nanometer range [1]. Owing to the rather large volume fraction of grain boundaries many physical properties are fundamentally changed in nanostructured materials. The driving forces of hydrogen in the grain boundary regions are of a particular importance in understanding of the hydriding mechanism.

In intermetallic compounds hydrogen atoms may occupy interstitial sites with different types of neighbouring atoms, and in nanocrystalline compounds a rather large quantities of hydrogen atoms may be located in the region of grain boundaries. However, the problem, how to organize an efficient supply of hydrogen into the regions which are able to accommodate, is not solved. There is experimental evidence [2] that the hydrogen diffusivity in nanocrystalline materials due to the existence of diffusion paths with reduced barrier height is

higher by an order of magnitude compared to that inside the crystalline grains.

Ball-milling technology is widely used to prepare Mg-based hydrogen absorbing nanocrystalline materials [3, 4]. Thin film physical vapour deposition technologies are emerging with nontraditional and new nanotechnology methods for designing high-performance storage materials [5, 6].

Physical vapour deposition technologies in combination with ion beam/plasma treatment technologies include many advantages in comparison with ball-milling technologies. Among the benefits of using physical vapour deposition technologies to prepare improved Mg-based materials there are: (i) the ease of formation of alloys and hydride phases at low temperatures; (ii) obtaining Mg-based materials in the nanocrystalline state, with various amounts of dislocations and special defects for hydrogen trapping; (iii) generation of highly reactive surfaces during the hydriding operation which increases the hydrogen adsorption efficiency.

In this paper, the hydriding behaviour of MgAl films prepared by physical vapour deposition in combination with plasma treatment technologies has been investigated. The emphasis is made on the study of surface effects initiated by incident ions extracted from plasma

in the mechanism of the formation of hydride phases and chemical compounds.

## 2. Experimental

In the vacuum chamber (0.5 m diameter and 1.2 m long) two cylindrical magnetrons (7.0 cm diameter) symmetrically surrounded the substrate holder that hosted samples  $1 \times 1 \text{ cm}^2$  in size made of stainless steel. The gap distance between magnetrons and sample was 7 cm. A dc discharge power supply was used to produce plasma that was independent from the plasma produced by the magnetrons. This independently generated plasma enveloped the sample holder, which was biased negatively, to perform the ion-sputter cleaning before the deposition and implantation of hydrogen during the deposition. The cathode of the magnetron was made of Mg and Al with a nominal purity better than 99.95 at. %.

All samples were ultrasonically cleaned using acetone then methanole. After having been cleaned, the samples were installed in the vacuum chamber. A typical argon sputter-cleaning process was used to remove the surface contaminants and the residual oxide. The magnetrons were not used in this process. A bias voltage of 100 V was applied to the sample holder. At the end of the sputter-cleaning process, after 15 min, the deposition of Mg and Al atoms process from separate and two independent magnetrons proceeded without any interruption. During deposition, the pressure of the argon working gas was stabilized at pressure 0.2 Pa, and power 500 W for Mg magnetron and power 600 W for Al magnetron were used. When a typical thickness of about 3–5  $\mu\text{m}$  was obtained (in approximately 10 min), the magnetrons were switched out, and the hydriding was conducted in hydrogen plasma. The supply of hydrogen was performed to keep the hydrogen working gas pressure equal to 10 Pa. After hydriding a thin about 20 nm thick Al layer was deposited on the top of the film. After exposure of samples in air, a thin 3–5 nm thick barrier layer of natural oxide  $\text{Al}_2\text{O}_3$  was formed on the surface that protected chemical compounds synthesized during hydrogenation from the direct contact with air and moisture. Then the samples were removed from the chamber and subjected to the structural and properties analysis.

In the present work the microstructure of films was analysed by X-ray diffraction with the  $2\theta$  angle in the range of  $20\text{--}90^\circ$  using  $\text{Cu } K_\alpha$  radiation in steps of  $0.05^\circ$ . The identification of phases has been performed using Crystallographic Search–Match program. The

scanning electron microscopy (JEOL JSM-6300) was used for the studies of surface morphology and topography on all stages of fabrication of thin films.

## 3. Results

### 3.1. X-ray diffraction study of MgAl films

The X-ray diffraction pattern of as-deposited MgAl film is shown in Fig. 1. The peaks are seen which belong to  $\text{Mg}_{17}\text{Al}_{12}$ . According to the Mg–Al binary phase diagram, the formation of  $\text{Mg}_{17}\text{Al}_{12}$  takes place when the fraction of Al dissolved in magnesium exceeds the solubility limit. Al is soluble in the hpc structure of Mg up to  $\sim 4.5$  at. % at  $250^\circ\text{C}$  [7]. The crystallite size and the strain were evaluated from the full width of half maximum of the reflection peaks. The crystallite

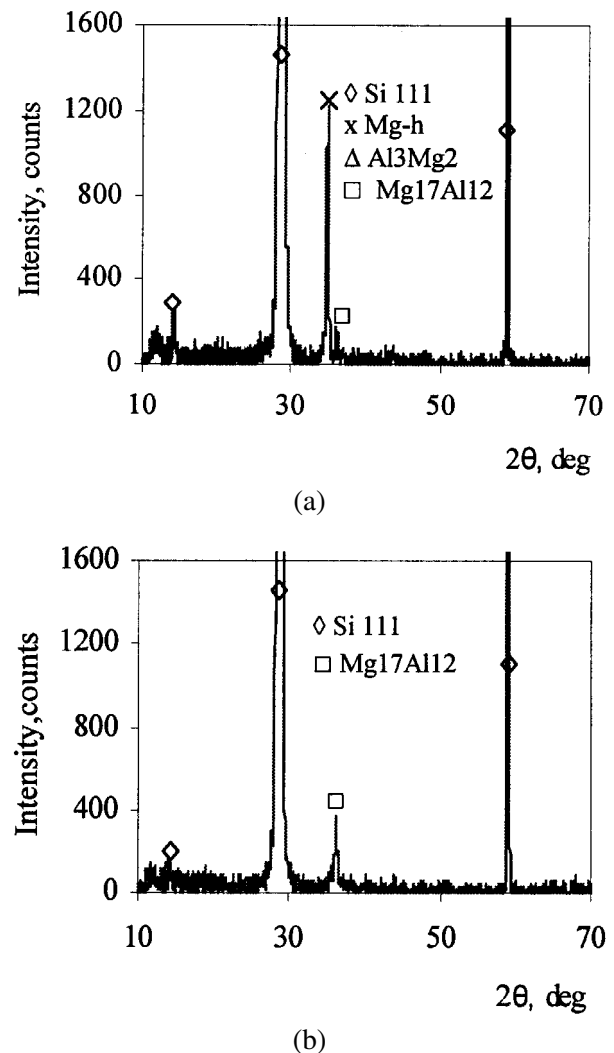


Fig. 1. XRD patterns of MgAl as-deposited for (a) Mg : Al = 80 : 20 and (b) Mg : Al = 60 : 40 films.

size and the strain reach about 65 nm and 0.25%, respectively.

As the Al content in film increases, the phase composition evolves from the almost pure hexagonal Mg to the  $Mg_{17}Al_{12}$ . The X-ray diffraction patterns of MgAl (80:20) film is shown in Fig. 1(a). The registered dominant phase is magnesium and the small amount of  $Mg_{17}Al_{12}$  can be distinguished. In the case of MgAl (60:40) (Fig. 1(b)), the dominant characteristic diffraction peak of  $Mg_{17}Al_{12}$  is observed. The various phases obtained in the MgAl compounds are close to those expected from the Mg–Al binary phase diagram [8]. The films of MgAl (60:40), which basically only contain a nanocrystalline  $Mg_{17}Al_{12}$  intermediate phase, have been used in plasma hydrogenation experiments.

### 3.2. Simultaneous deposition and hydrogenation

The XRD patterns of MgAl (60:40) films hydrogenated by hydrogen ion irradiation during deposition at 80 °C under floating substrate potential (Fig. 2(a)) and the negative bias voltage 100 V (Fig. 2(b)) are shown in Fig. 2. It is seen that the synthesis reaction which results in the formation of  $Mg(AlH_4)_2$  has occurred. The small amounts of tetragonal  $MgH_2$ ,  $Mg_{17}Al_{12}$ , and Al are registered after hydriding under the floating substrate potential (Fig. 2(a)). The X-ray diffraction patterns of the films hydrogenated under the negative bias voltage 100 V were recorded to identify the complete transformation of the  $Mg_{17}Al_{12}$  phase into  $Mg(AlH_4)_2$  (Fig. 2(b)).

Thus, the hydrogen ion implantation during MgAl film deposition leads to the following reaction:



The decomposition of magnesium alanate starts at temperature above 80 °C [6]. The decomposition reaction can be written as

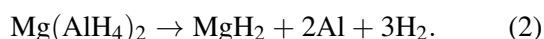
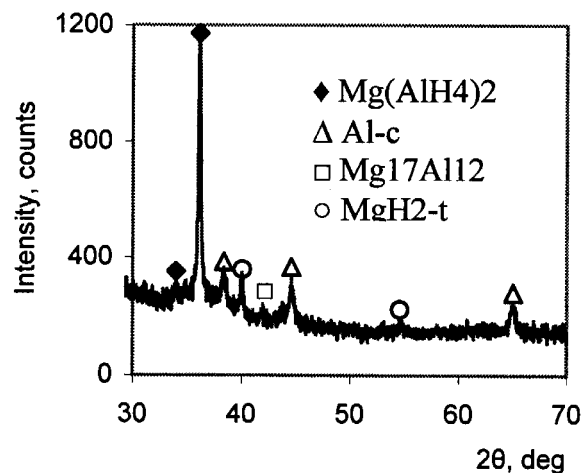


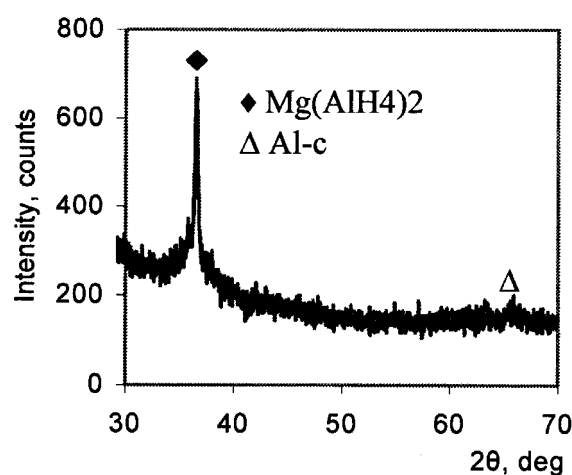
Figure 3 includes SEM surface views of as-deposited film hydrogenated during deposition at the temperature of 80 °C (Fig. 3(a)) and after the thermal annealing at the temperature 200 °C (Fig. 3(b)). The released hydrogen forms bubbles, and metallic Al forms randomly distributed crystallites.

### 3.3. Hydrogenation in $H_2+Ar$ plasma

The 5  $\mu m$  thick  $Mg_{17}Al_{12}$  films deposited on a silicon (111) substrate were hydrided in  $H_2+Ar$  (30%  $H_2+70%$  Ar) working gas ( $p \approx 1$  Pa) plasma in the



(a)



(b)

Fig. 2. XRD patterns of MgAl films hydrogenated during deposition at 80 °C (a) under the substrate floating potential and (b) under the negative 100 V bias voltage.

same vacuum chamber without exposure in air. The incident Ar ions extracted from plasma have energies about 100 eV and are able to initiate displacement of surface atoms, resulting in formation of surface vacancies and adatoms, and sputtering processes, while incident hydrogen ions predominantly penetrate in subsurface layer of film losing their energy through electronic interactions and related processes.

Figure 4 includes the XRD patterns of  $Mg_{17}Al_{12}$  films after hydriding in 30%  $H_2+70%$  Ar working gas plasma at total pressure about 1 Pa and temperature 80 °C for 5 min under the substrate floating potential (Fig. 4(a)) and under the negative bias voltage equal to 100 V (Fig. 4(b)). It is seen that the initially homogeneous as-deposited  $Mg_{17}Al_{12}$  film, after 5 min hydriding in  $H_2+Ar$  plasma, includes phases of  $Mg(AlH_4)_2$ ,  $MgH_2$ , and Al. The small amount of  $Mg_2Al_3$  is not

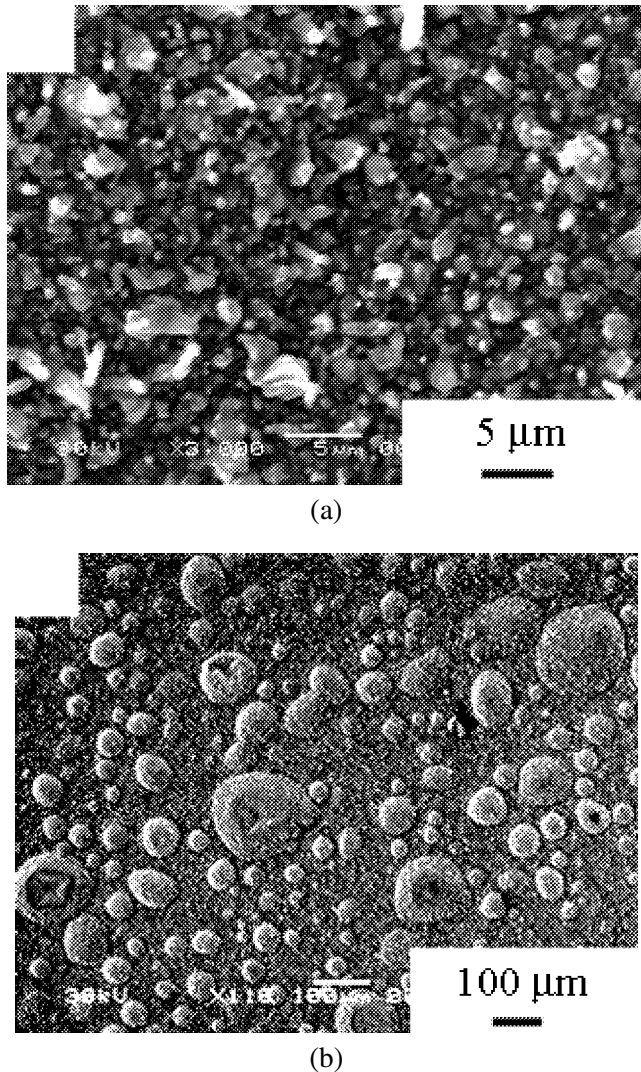
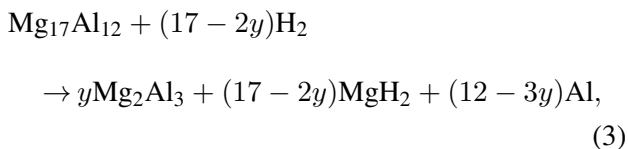


Fig. 3. SEM surface views of (a) MgAl films hydrogenated during deposition at 80 °C and (b) after the thermal annealing at 200 °C for 5 min.

excluded. The hydriding under the negative bias voltage 100 V (Fig. 4(b)) shows that the fractions of MgH<sub>2</sub> and Al increase while the characteristic diffraction line of the magnesium alanate is considerably reduced. The hydriding reaction in H<sub>2</sub>+Ar plasma under 100 V negative bias voltage can be written as [9]



where the value of  $y$  can be obtained through an evaluation of the proportion of phases, which is beyond the scope of this work.

The SEM surface topography analysis shows that initially smooth as-deposited Mg<sub>17</sub>Al<sub>12</sub> film (Fig. 5(a))

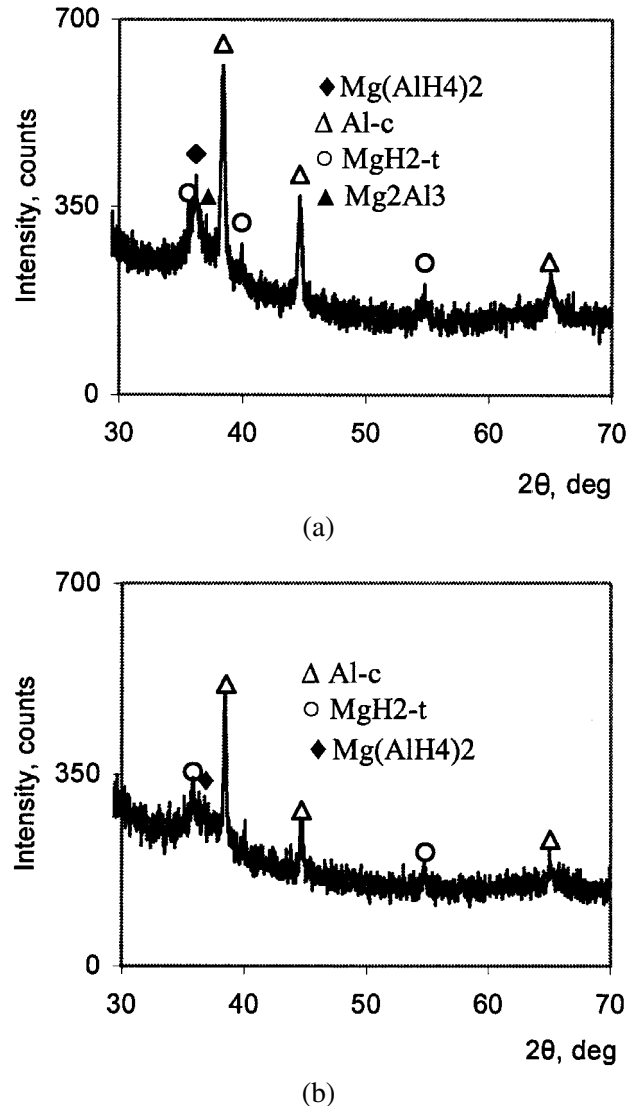
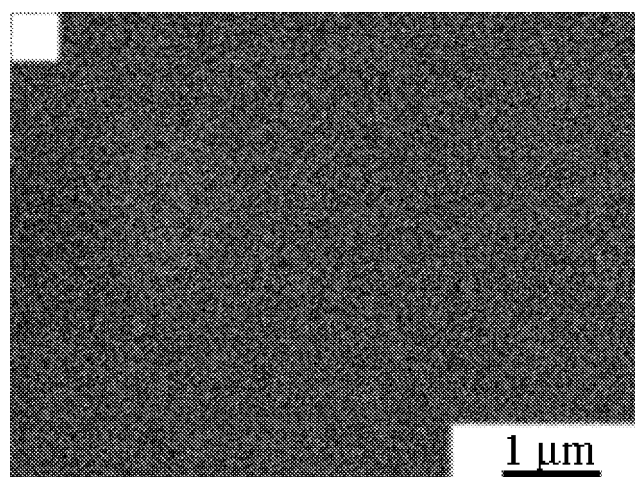


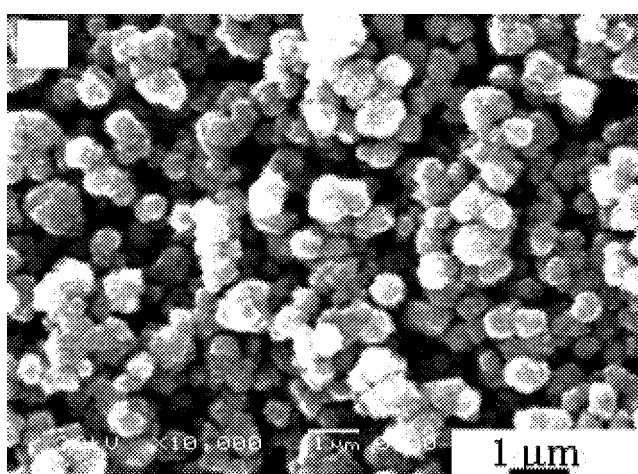
Fig. 4. XRD patterns of Mg<sub>17</sub>Al<sub>12</sub> films after hydrogenation in H<sub>2</sub>+Ar plasma at 80 °C (a) under the substrate floating potential and (b) under the negative 100 V bias voltage.

becomes rough and includes microformations which can be interpreted as new phases in plasma hydrogenated film (Fig. 5(b)).

After thermal annealing of Mg<sub>17</sub>Al<sub>12</sub> films hydrogenated in H<sub>2</sub>+Ar plasma, the intermetallic Mg<sub>17</sub>Al<sub>12</sub> phase is recovered. Figure 6 illustrates an XRD diffractogram of the MgAl film hydrogenated in H<sub>2</sub>+Ar plasma during 5 min at 80 °C under 100 V bias voltage and afterwards annealed in vacuum at 230 °C for 5 min. It seems that reactions taking place during hydrogenation are reversible during the thermal annealing with recovery of the starting Mg<sub>17</sub>Al<sub>12</sub> phase.



(a)



(b)

Fig. 5. SEM surface views of  $Mg_{17}Al_{12}$  films (a) as-deposited and (b) after plasma hydrogenation.

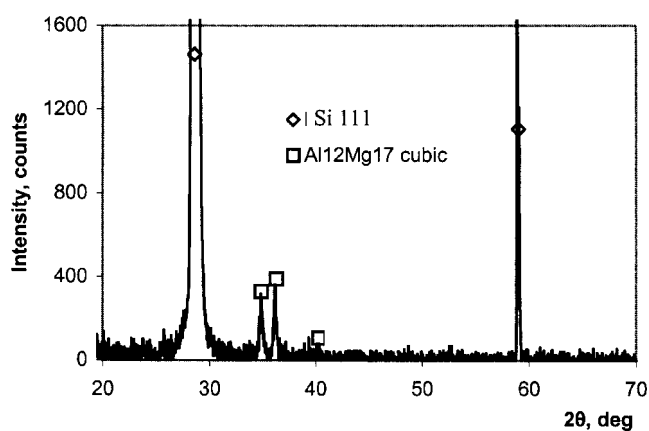


Fig. 6. XRD patterns of  $Mg_{17}Al_{12}$  film hydrogenated in plasma at  $80\text{ }^{\circ}\text{C}$  after the thermal annealing at  $230\text{ }^{\circ}\text{C}$  for 5 min.

#### 4. Discussion

There have been a number of studies in the literature that have focused on the kinetics of hydrogen sorption in Mg and Mg alloys [10]. It is agreed that at the beginning of the hydriding reaction, the reaction is controlled by the direct chemical reaction between hydrogen and the exposed metal surface. After surface is covered by a hydride layer, the hydriding kinetics is controlled by the supply rate of reaction products from the surface into the bulk [11]. Hydrogenation during film growth by hydrogen ion implantation changes the synthesis kinetics. The synthesis reaction between hydrogen and adsorbed Mg and Al atoms is controlled by the fluxes of incident reacting species and reaction kinetics.

The surface chemistry is directed to optimize bondings between reacting species and it results in surface diffusion over distances of many atomic bonds. External ion irradiation intensifies intermixing of metal atoms, adsorbed species, and incident ions. A thin layer enriched by incident reactive particles is formed on the surface. The concentration of the reactive species in this layer reaches steady state in 10–20 s for the irradiation conditions used in the present work [12]. The steady state concentration of reactive species in growing film depends on the deposition and surface erosion rates. The quantitative evaluations made on the basis of the model published in [13] show that concentration of hydrogen exceeds the concentration of matrix atoms 6–8 times and the synthesis kinetics was not retarded by hydrogen supply rate.

Different physical phenomena take place under high-flux, low-energy  $H_2+Ar$  ion irradiation of  $Mg_{17}Al_{12}$  film. The incident hydrogen ions saturate surface layer with hydrogen. The maximum hydrogen concentration in it can be evaluated as  $N/Y$ , where  $N$  is the concentration of matrix atoms and  $Y$  is the sputtering yield. The sputtering yield for 100 eV  $Ar^+$  is about 1 for metal targets. In this way, the hydrogenation of MgAl film in  $H_2+Ar$  plasma leads to the formation of highly activated layer on the surface with the concentration of hydrogen which is insufficient for the transformation of MgAl film into magnesium alanate. The activated metal atoms cluster into  $Mg_2Al_3$  and Al phases. The incorporated free hydrogen reacts with magnesium forming  $MgH_2$ . This model explains the observation of  $MgH_2$ ,  $Mg_2Al_3$ , and Al phases in XRD patterns of plasma hydrogenated  $Mg_{17}Al_{12}$  films.

However, the mean penetration depth of 100 eV  $H^+$  is equal to about  $0.5\text{ }\mu\text{m}$  [14]. The transformation of  $5\text{ }\mu\text{m}$  thick  $Mg_{17}Al_{12}$  into the new phase film cannot

proceed without the process of long-range atom transport from the surface into the bulk and restructuring. An attempt to explain these processes is made as follows.

The heterogeneous processes on the surface result in that the plasma-activated surface layer is both chemically and physically distinct from the lying bulk material. The difference in chemical potentials between the activated surface, bulk, and grain boundaries is established. It is shown [15] that the excess chemical potential of the surface relative to grain boundaries produces a net flow from the surface of metal atoms and adsorbed species into the grain boundaries that generates compressive stress in grains. Grain boundaries become saturated with hydrogen atoms. When the stress exceeds the plasticity, the stress relaxation occurs through the emission of dislocations and the formation of subgrains within the original grain structure takes place. In this way the uptake of hydrogen through the grain and subgrain boundaries in open contact with the highly hydrogen enriched activated surface layer occurs. The intensive intermixing of atoms within the grains with continuous supply of hydrogen through the boundaries takes place resulting in the synthesis of new phases and compounds.

Sputtering during hydriding in  $H_2+Ar$  plasma limits the supply rate of hydrogen through the grain boundaries from the surface into the bulk. The synthesis of magnesium alanate is retarded. It was shown [6] that hydriding in pure  $H_2$  plasma, when sputtering can be neglected, results in the complete transformation of  $Mg_{17}Al_{12}$  into magnesium alanate. Hydriding in  $H_2+Ar$  plasma under floating potential results in  $Mg(AlH_4)_2$ ,  $MgH_2$ , and Al phases. The magnesium alanate disappears after hydriding under 100 V bias voltage.

These results are in qualitative agreement with the results of the studies of the structure and hydrogen adsorption properties of MgAl alloys prepared from mixtures of pure elemental Mg and Al powder by high-energy ball-milling [16]. Ball-milling leads to continuous creation of fresh surfaces as result of fragmentation of crystallites induced by high load stress and deformation at the interfaces of the colliding particles. These conditions result in a very enhanced local reactivity, and allow the reagents to form the compounds. It is shown that in the case of MgAl (58:42), which after ball-milling basically only contains a nanocrystalline  $Mg_{17}Al_{12}$  intermetallic phase, hydriding leads to the formation of  $MgH_2$  and Al. However, if the hydriding employing ball-milling takes place at high hydrogen pressure of thermally (350–400 °C) activated pow-

der [9] the hydriding in  $H_2$  and  $(Ar+H_2)$  plasmas takes place at temperature 70 °C. The high temperature of hydriding used in the ball-milling technology to support the kinetics of hydrogen supply into the reaction zone excludes the synthesis possibility of the  $Mg(AlH_4)_2$  compound.

One possible interpretation is that the transported species are a more mobile hydride, such as  $AlH_3$  [11]. The low melting point of  $Mg(AlH_4)_2$  demonstrates the weak nature of the ionic bond. It is possible that disintegration of  $Mg(AlH_4)_2$  into  $MgH_2$  and  $AlH_3$  takes place.  $AlH_3$  is then transported to the site where it reacts with  $MgH_2$  forming  $Mg(AlH_4)_2$  (low temperature case) or dissociates into Al and  $H_2$  (elevated temperature case).

## 5. Conclusions

The MgAl films were hydrogenated in two ways: (i) deposition of Mg and Al atoms during simultaneous hydrogen ion implantation, and (ii) plasma hydrogenation of  $Mg_{17}Al_{12}$  films under high-flux, low-energy ion irradiation. Hydrogen incorporated in the growing film reacts with adsorbed metal atoms and takes part in the synthesis reaction of magnesium alanate at a temperature below 80 °C. At higher temperatures, the decomposition of magnesium alanate starts.

Hydrogenation kinetics of MgAl films in  $H_2+Ar$  plasma is limited by the supply rate of hydrogen from the surface into the bulk. It is suggested that sputtering is the dominant process that limits the concentration of hydrogen on the surface.

## Acknowledgements

This work was performed under support from the Hydrogen Program of the US Department of Energy and the Sandia National Laboratories. Authors express special gratitude to Mr. A. Vasys (USA) for the encouragement and help in an administration of the research.

## References

- [1] G. Majer, U. Eberle, F. Kimmerle, E. Stanik, and S. Orimo, Hydrogen diffusion in metallic and nanostructured materials, *Physica B* **328**, 81–89 (2003).
- [2] R. Haugsrud, On high temperature oxidation of nickel, *Corrosion Science* **45**, 211–235 (2003).
- [3] S. Orimo, K. Ikeda, H. Fujii, Y. Fujikawa, Y. Kitano, and K. Yamamoto, Structural and hydriding properties of the Mg–Ni–H system with nano- and/or amorphous structures, *Acta Mater.* **45**, 2271–2278 (1997).

- [4] L. Zaluski, A. Zaluska, and J.O. Strom-Olsem, Hydrogen absorption in nanocrystalline  $Mg_2Ni$  formed by mechanical alloying, *J. Alloys Comp.* **217**, 245–249 (1995).
- [5] K. Higuchi, K. Yamamoto, H. Kajioka, K. Toiyama, M. Honda, S. Orimo, and H. Fuji, Remarkable hydrogen storage properties in three-layered Pd/Mg/Pd thin films, *J. Alloys Comp.* **330–332**, 526–530 (2002).
- [6] L. Pranevicius, D. Milcius, L.L. Pranevicius, and G. Thomas, Plasma hydrogenation of Al, Mg and MgAl films under high-flux ion irradiation at elevated temperature, *J. Alloys Comp.* **373**, 9–15 (2004).
- [7] H.P. Klug and L.E. Alexander, *X-ray Diffraction Procedures for Polycrystalline and Amorphous Materials* (Wiley, New York, 1974).
- [8] A.A. Nayeb-Hashemi and J.B. Clark (eds.), *Phase Diagrams of Binary Magnesium Alloys* (ASM International, 1998).
- [9] S. Bouaricha, J.P. Dodelet, D. Guay, J. Huot, S. Boily, and R. Schultz, Hydriding behavior of Mg–Al and leached Mg–Al compounds prepared by high-energy ball milling, *J. Alloys Comp.* **297**, 282–293 (2000).
- [10] K.J. Gross, E.H. Majzoub, and S.W. Spangler, The effects of titanium precursors on hydriding properties of alanates, *J. Alloys Comp.* **356–357**, 423–428 (2003).
- [11] K.J. Gross, S.E. Guthrie, S. Takara, and G.J. Thomas, *In-situ* X-ray diffraction study of the decomposition of  $NaAlH_4$ , *J. Alloys Comp.* **297**, 270–281 (2000).
- [12] D. Milcius, C. Templier, J.-P. Riviere, L.L. Pranevicius, and L. Pranevicius, High-flux, low-energy implantation effects on the composition of the altered layer, *Surf. Coating Technol.* **156**(1–3), 214–218 (2002).
- [13] L. Pranevicius, C. Templier, J. Delafond, and S. Muzard, Simulation of interface effects during simultaneous deposition and ion irradiation, *Surf. Coating Technol.* **72**, 51–61 (1995).
- [14] L. Pranevicius, *Coating Technology: Ion Beam Deposition* (Satas & Associates, Warwick, 1993).
- [15] P. Fielitz, G. Borcardt, M. Schmücker, H. Schneider, and P. Willich, Measurement of oxygen grain boundary diffusion in mullite ceramics by SIMS depth profiling, *Appl. Surf. Sci.* **9248**, 1–5 (2002).
- [16] S. Bouaricha, J.P. Dodelet, D. Guay, J. Huot, S. Boily, and R. Schulz, Hydriding behavior of Mg–Al and leached Mg–Al compounds prepared by high-energy ball-milling, *J. Alloys Comp.* **297**, 282–293 (2000).

## MgAl PLĖVELIŲ SODRINIMAS VANDENILIU PLAZMOJE

L. Pranevičius<sup>a</sup>, D. Milčius<sup>b</sup>, L.L. Pranevičius<sup>a,b</sup>

<sup>a</sup> Vytauto Didžiojo universitetas, Kaunas, Lietuva

<sup>b</sup> Lietuvos energetikos institutas, Kaunas, Lietuva

### Santrauka

MgAl plėvelių sodrinimo vandenilio atomais ir molekulėmis kinetikos tyrimas buvo atliktas dviem būdais: a) implantuojant vandenilio jonus su energija 100 eV į augančią plėvelę, ir b) apspinduliuavus  $Mg_{17}Al_{12}$  plėvelę intensyviais mažų energijų vandenilio jonų srautais panaudojant  $H_2+Ar$  plazmą. Faziniai ir struktūriniai virsmai plėvelėse buvo tiriami  $\gamma$  spindulių difraktometru, o paviršiaus morfologija – skenuojančiu elektroniniu mikroskopu. Rasta, kad MgAl plėvelėse, nusodintose su vienalaikė vandenilio jonų implantacija, dominuoja  $Mg(AlH_4)_2$  cheminis junginys, kuris susiskaido

į  $MgH_2$  ir Al prie didesnių nei 80 °C temperatūrų. Plėvelėse, kurios buvo sodrinamos vandeniliu panaudojant joninę spinduliuotę iš  $H_2+Ar$  plazmos, rasti  $Mg(AlH_4)_2$ ,  $MgH_2$ ,  $Mg_2Al_3$  ir Al dariniai. Daroma išvada, kad joninės spinduliuotės metu Ar jonai riboja vandenilio įtekėjimą į medžiagos tūrį, o tuo pačiu ir sintezės reakciją.

Stebėti eksperimentiniai rezultatai aiškinami, padarius prielaidas apie atomų judėjimą dideliais atstumais sodrinimo metu ir tarpkristalinės masės pernašos nanokristalinėse plėvelėse svarbią įtaką hidridų susidarymo mechanizmui.